Enhancing Photovoltaic Performance Using Solar Reflectors and Active Cooling in Hot Climates

Youssef Kassem
Department of Mechanical Engineering, Engineering Faculty, Near East University, Nicosia (via Mersin 10, Turkiye), Cyprus | Energy, Environment, and Water Research Center, Near East University, Nicosia (via Mersin 10, Turkiye), Cyprus
yousseuf.kassem@neu.edu.tr (corresponding author)

Huseyin Camur
Department of Mechanical Engineering, Engineering Faculty, Near East University, Nicosia (via Mersin 10, Turkiye), Cyprus
huseyin.camur@neu.edu.tr

Huseyin Gokcekus
Department of Civil Engineering, Civil and Environmental Engineering Faculty, Near East University, Nicosia (via Mersin 10, Turkiye), Cyprus | Energy, Environment, and Water Research Center, Near East University, Nicosia (via Mersin 10, Turkiye), Cyprus
huseyin.gokcekus@neu.edu.tr

Mustapha Tanimu Adamu
Department of Mechanical Engineering, Engineering Faculty, Near East University, Nicosia (via Mersin 10, Turkiye), Cyprus
mustaphatanimu.adamu@neu.edu.tr

Ibrahim Aliyu Tukur
Department of Mechanical Engineering, Aliko Dangote University of Science and Technology, Wudil, Nigeria
ibrahimatukur83@gmail.com

Received: 6 January 2026 | Revised: 9 February 2026 | Accepted: 14 February 2026

 DOI: https://doi.org/10.48084/etasr.17386

ABSTRACT

This study experimentally evaluates a hybrid approach to improving the optical and thermal performance of Photovoltaic (PV) modules operating in hot-climate conditions. The main objective is to reduce efficiency losses caused by high temperatures under maximum Solar Radiation (SR) using a common side reflector and an active water-cooling method. Outdoor experiments were conducted in Kano State, Nigeria, where three 10W polycrystalline PV cell configurations (a reference module, a reflector-assisted module, and a reflector-assisted module with active water cooling) were used. All systems were analyzed based on output power, unit Surface Temperature (ST), SR, and Solar Hour Angle (SHA). The results showed that the reflector-only configuration increased incident SR by up to 47%, at the expense of a matching increase in ST by up to 29%. In contrast, the combined reflector–cooling configuration resulted in a temperature increase of up to 15% while maintaining radiation gains, thus recording the highest net power output. The comparative analyses prove that thermal regulation is necessary to realize the full optical enhancement benefit. Moreover, a scaling analysis demonstrates the applicability of the proposed approach, which yields roughly 187 MWh of energy annually for a 1000 m² installation in northern Nigeria. Consequently, the outcomes demonstrate that combining active cooling and optical concentration is an effective method to increase PV efficiency, especially in hot regions.

Keywords-Nigeria; photovoltaic systems; solar reflectors; active cooling; solar hour angle; power output enhancement

I. INTRODUCTION

PV systems have become the most advanced renewable energy technology due to the increasing need for clean energy. Although their benefits, including minimal maintenance costs and ease of installation, are significant, environmental conditions, such as temperature, dust accumulation, and shading, pose serious challenges to PV system performance. Innovative methods for improving the performance of PV and Photovoltaic/Thermal (PVT) systems have been explored. In general, cooling systems are one of the main methods for improving the efficiency of PVT systems. They can lower the operating temperature of solar cells and increase both thermal and electrical efficiency. Various water-based and air-based cooling techniques have been examined, including solar air collectors with finned systems [1, 2], optimized air gap systems [3], bi-fluid-based air and nanofluid combinations [4], double pass and channel-based heat exchangers [5, 6], partially and fully cooled systems [7], and direct contact-based water cell systems [8]. Additionally, several studies have focused on material development and/or selection to enhance heat transfer and thermal regulation in PVT systems. This includes a composite sorption material with increased thickness for improved PV cooling systems [9] and a low-cost PVT heat exchanger made from polypropylene, with promising potential for both efficiency and cost-effectiveness [10]. Moreover, optimization-based approaches have gained popularity for determining the optimal design and operating parameters of PVT systems. These approaches include numerical optimizations of design parameters such as fins for phase change material-based cooling systems [11], Multiphysics and parametric sensitivity studies to ascertain and rate the governing factors affecting the performance of PVT systems, and multi-criteria-based evaluations considering parameters such as energy, exergy, environmental, and economic aspects [12]. Additionally, review studies have integrated optimization-based approaches, providing comprehensive and systematic comparisons of conventional and alternative PV and PVT systems, as well as current trends and challenges associated with PVT systems and their variants [13]. Besides, the role that optical enhancement technologies, specifically solar reflectors, play in increasing the amount of SR incident on both PV and PVT systems has been investigated. Authors in [14] analyzed the combined effects of different reflector configurations and cooling flow fields. Authors in [15] demonstrated the importance of optimized cooling to mitigate thermal penalties associated with reflector-assisted PV systems. Authors in [16] concluded that integrating reflectors may also enhance the performance of finned passive PVT systems. Authors in [17] discussed the status of reflectors as one of the key performance enhancement approaches, along with cooling media and economic consideration aspects. Authors in [18] showed that shiny aluminum and mirror reflectors increased PV power output by 30% and 33%, respectively, and also led to ST increases of up to 10 °C. The reflector material, tilt angle, and orientation are crucial to performance gains, with optimal tilt angles between 60° and 75° [19, 20]. V-trough and bi-reflector configurations, such as those of [21, 22], further enhanced irradiance, thereby yielding power output increases of over 25%. The tracking systems enhance the reflectors' efficiency. According to [23], the efficiency of a one-axis three-position tracking system with a low-concentration reflector configuration can boost panel efficiency by 56% compared to a fixed PV panel arrangement. Solar reflectors have attracted attention for their ability to enhance PV and PVT systems. Figure 1 shows previous studies on enhancing the performance of PV/PVT systems using reflectors and coolant in Nigeria.

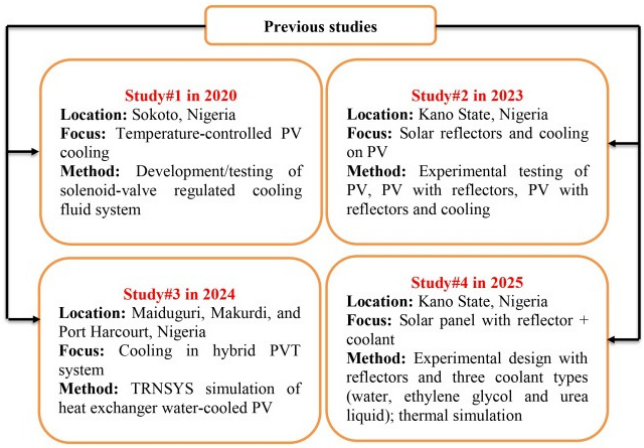

Fig. 1. Studies related to enhancing the performance of PV/PVT using a reflector and coolant in Nigeria.

As depicted in Figure 1, few studies have been conducted to enhance PV performance under Nigeria's climatic conditions, with most investigations focusing on cooling systems or reflectors in PV systems. In addition, there is a lack of long-term experimental studies concerning the combination of optical enhancement and active cooling by using low-cost materials [24-27]. Consequently, the relevance and importance of this research lie in its effort to provide adequate solutions to some of the biggest challenges that have hindered PV conversion efficiency to date, including efficient heat rejection through cooling. Therefore, the performance improvement of PV systems achieved by the combined application of solar reflectors and an active water-cooling technique is experimentally investigated in this study through a long-term outdoor experimental campaign. The independent and combined effects of reflector-assisted irradiance enhancement and active thermal regulation on the generated electrical power, ST, and overall efficiency of polycrystalline silicon-based solar power systems are evaluated. The experimental study is carried out in Kano State, Nigeria. The specific location is representative of a hot, high-irradiance, and dusty environment, suitable for various regions in Sub-Saharan Africa. Additionally, a comparative study is conducted over six months between a conventional PV system, a reflector-assisted PV system, and a reflector-assisted cooled PV system. This research seeks to contribute to the development of empirical data on cost-effective PV performance enhancement measures applicable in developing countries. Such data are widely expected to be useful in ensuring more efficient PV

applications in buildings, medical facilities, and other infrastructure with high energy demand operating under extreme weather conditions.

II. CASE STUDY

A. Experimental Setup

The experimental work was carried out in Kano State, Nigeria. This location is characterized by high SR and ambient temperature, making it suitable for testing the efficacy of methods that improve the performance of PV systems. The experimental arrangement was erected on the rooftop of the Oriental Hospital, Tarauni Local Government Area, Kano State, Nigeria, in an open-sky configuration. The experiment was conducted from October 2021 to March 2022. During this period, the region experienced high SR, low rainfall, and the possibility of Harmattan winds in northern Nigeria. In this study, three identical polycrystalline modules of a power rating of 10W were used. The solar modules were placed Facing South at a fixed tilt angle that corresponds to the latitude of Kano State. The electrical parameters under Standard Test Conditions (STC) are given in Table I. K-type thermocouples with an accuracy of ±0.5 °C were utilized to measure the PV module ST and water temperature. Incident SR was measured by a Dynalab pyranometer, with a measurement uncertainty of ±5 W/m². The electrical parameters, such as voltage and current, were monitored using a DC voltmeter and an ammeter, with accuracies of ±0.5% and ±0.5%, respectively. The cooling water flow rate was measured by utilizing a calibrated flow meter with an uncertainty of ±2%. To investigate the effects of optical concentration and thermal management, three PV configurations were considered (Configuration#1: Panel without modification, reference case; Configuration#2: Panel with side reflectors; and Configuration#3: Panel with side reflectors and a water-cooling system), as shown in Figure 2.

TABLE I. SPECIFICATION OF THE SELECTED SOLAR PANEL

Specification	Unit	Value/type
Panel type		Poly crystalline
Maximum power	W	10
DC open circuit voltage	V	21.8
DC max power current	A	17.3
Normal ST	℃	25
Panel size	mm	350×300×25
Life span	Year	25

Fig. 2. Three PV configurations are considered in the current study.

B. Reflector Design

In [28], a schematic illustration of a V-trough concentrator was presented. The Concentration Ratio (CR) is the primary design parameter of a V-trough system. The concentrator geometry is defined by several parameters, including the acceptance angle (α), the trough angle (Ψ), the collector aperture width (A), the receiver base width (B), and the slant height of the reflector (H). Among these parameters, the acceptance angle (α) and the trough angle (Ψ) mainly determine the CR. A V-trough concentrator can be designed using different models depending on the operating conditions and the required CR. Detailed descriptions of these models are available in [29]. In the present study, the V-trough geometry was designed using the model proposed in [30]:

$$CR = \frac{\sin[(2n+1)\psi+\alpha]}{\sin(\psi+\alpha)} \quad (1)$$

$$\frac{H}{B} = \frac{\sin((2n+1)\psi+\alpha)-\sin(\psi+\alpha)}{2\sin(\psi+\alpha)\sin\psi} \quad (2)$$

where n is the number of reflections from the reflector before reaching the receiver.

The width of the receiver base, B, was limited in the current V-trough design. Since a higher slope height also results in a higher vertical height, the slope height of the reflector, as demonstrated in (2), H, was required to remain below 35 cm. This limitation is in place to prevent the concentrator V-trough module from becoming bulky by keeping its volume as minimal as possible. Consideration is also given to the concentrator module's manufacturability from the perspective of solar cells. The accessibility of commercial solar cells limited the utility of B.

The reflector tilt angle α was optimized to 30°, corresponding to a CR of approximately 2 under normal solar incidence. Through optimization, the reflector length was determined to be 35 cm to achieve maximum irradiance enhancement without excessive shading. Moreover, flat reflectors were made with a commercially available aluminum sheet of 0.5 mm thickness. The reflectivity of the aluminum surface was measured with an albedo meter, which indicated an albedo of around 98%. The amount of SR concentrated on the PV module surface was highly dependent on the concentration ratio. As the CR increased, the PV module's electrical power output and efficiency increased due to the higher incident solar irradiance. The V-trough reflector under consideration in this study is predicated on optimum surface reflectivity and diffuse reflection. Surface roughness, dust accumulation on the reflector surface, surface oxidation of the reflector material, and structural mismatches at the incidence angle of solar rays can all cause optical losses in outdoor settings under SR. In addition to the effects of reflector-assisted PV panel systems, an uneven distribution of SR can be experienced across the PV cell surface. Gradients in temperature may eventually arise from this. Seasonal fluctuations in SR may also impact the CR of solar concentrators.

C. Cooling System Design

In Configuration#3, as depicted in Figure 3, an S-shaped copper tube was attached to the rear surface of the PV panel, and an active cooling system was implemented. The tube had an internal diameter of 7 mm and a total length of 2.5 m. Water

was used as the cooling medium because it is readily available and has a relatively high thermal capacity. This design choice is supported by an analysis of the Reynolds number (Re), which provides a robust justification for its selection. Re is a dimensionless parameter that characterizes the fluid flow regime within the cooling system. It is calculated by [31]:

$$\mathrm{Re} = \frac{\rho V L}{\mu} \quad (3)$$

where ρ is the water density (998 kg/m^3), V is the fluid velocity (0.425 m/s), L is the characteristic length of the tube (2.5 cm), and μ is the dynamic viscosity of the fluid (1.002×10^{-3} Pa.s). Based on these parameters, since Re>4000, indicating the presence of fully turbulent flow conditions [32].

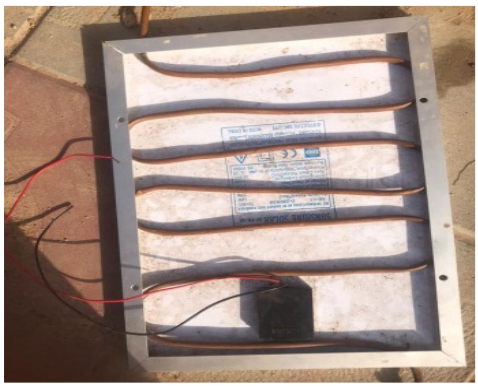

Fig. 3. The panel with the cooling system.

The choice of the S-shaped copper pipe introduces a unique geometric configuration into the cooling system, which significantly influences the cooling fluid's flow regime and pattern. Re, a significant parameter in fluid dynamics, is used here as a design criterion to elucidate the impact of this choice. The S-shape design is characterized by bends and curves that induce turbulence in the flow since Re>4000. Turbulence enhances heat transfer by increasing convective heat transfer between the cooling fluid and the panel's surface. This promotes more efficient cooling and contributes to superior thermal management [33]. Furthermore, the extended heat exchange path afforded by the S-shape design augments its effectiveness in. On the other hand, turbulence introduces additional hydraulic losses that must be accounted for when performing a complete thermal–hydraulic assessment.

The pressure drop in the cooling tube can be determined using the Darcy-Weisbach equation [31]:

$$\Delta P = f\frac{L}{D}\frac{\rho V^2}{2} \quad (4)$$

where ΔP is the pressure drop, f is the friction factor, L is the tube length, and D is the tube diameter.

For turbulent flow in smooth copper tubes, the friction factor can be approximated using the Blasius correlation [34]:

$$f = 0.316\mathrm{Re}^{-0.25} \quad (5)$$

The hydraulic pumping power (P_{pump}) required to circulate the cooling water can be estimated as a function of pressure drop (ΔP) and volumetric flow rate (Q), as given in [31]:

$$P_{pump} = \Delta P \times Q \quad (6)$$

The use of turbulent flow for active cooling achieves a substantial net energy benefit because the electrical power required to operate the pump is relatively small compared to the increase in electrical power output resulting from improved PV cell cooling [35-38]. Therefore, the estimated pumping power may be negligible relative to the increase in electrical power resulting from efficient thermal regulation of the PV cell module surface.

D. Temperature-Induced Power Loss Estimation

The temperature coefficient of power, a commonly used technique for analyzing the performance of PV modules, has been used to estimate the reduction in electrical power output due to temperature increases. It has been demonstrated that the electrical power production of PV modules is proportional to the cell temperatures [39, 40].

Therefore, the power loss percentage in PV modules can be expressed as [41]:

$$\Delta P(\%) = \gamma(T_{PV} - T_{ref}) \quad (7)$$

where γ is the Temperature Coefficient (%/°C), T_{PV} is the measured PV ST under a given configuration, and T_{ref} is the PV ST of the reference (unmodified) module.

E. Multiple Linear Regression (MLR)

MLR is utilized to describe the relationship between the dependent variable (output power Energy Production (EP) and independent variables, including Month Index (MI), SR, and ST. MLR can be expressed as [42]:

$$y_i = \beta_0 + \beta_1 x_1 + \cdots + \beta_i x_i \quad i = 1,2 \ldots n \quad (8)$$

where y_i represents the dependent variable (P_{output}), x_i where i=1,2…n, represents the independent variables, and β is called the intercept. IBM SPSS Statistics 20 is used to develop the regression model.

F. Experimental Results

Table II presents the descriptive statistics of configuration, including mean, Standard Deviation (SD), Maximum (Max) value, and Minimum (Min) value. The mean value of SR was found to be within the range of 431.3 W/m^2 -888.2 W/m^2. The Max and Min mean values were achieved in March for Configuration #3 and in January for Configuration #1. Configuration#2 recorded the highest mean ST value of 74.98 °C in March, while Configuration#1 recorded the lowest mean ST value of 41.16 °C in February. Moreover, the lowest mean EP value of 5.26 W was recorded in January for Configuration #1, and the highest value of 8.60W was reported in March for Configuration #3. Furthermore, the variation of SR values with various SHA during the investigation period is illustrated in Figure 4.

TABLE II. DESCRIPTIVE STATISTICS OF SR, ST, AND EP DATA

Configuration	Month	SR [W/m²]				ST				EP [W]			
		Mean	SD	Min	Max	Mean	SD	Min	Max	Mean	SD	Min	Max
Configuration#1	October	485.6	157.4	294	718	45.93	12.64	25.9	60.4	5.6	1.41	3.82	7.57
	November	514.9	148.5	315	728	49.02	13.03	26.7	63.7	6.13	1.38	4.31	8.18
	December	466.6	147.0	266	677	44.3	12.97	22.4	58.7	5.67	1.45	3.74	7.83
	January	431.3	159.8	193	673	43.21	12.45	23.1	59.1	5.26	1.60	2.78	7.61
	February	445	155.9	217	678	41.16	14.04	16.5	58.2	5.3	1.55	2.97	7.61
	March	521.3	151.6	321	731	49.63	12.99	27.5	64.2	5.93	1.4	4.06	7.91
Configuration#2	October	820	253	504	1160	69.37	19.06	39.2	91.2	7.63	1.68	5.45	9.97
	November	880.8	254.4	539	1246	71.37	18.99	38.9	92.7	8.01	1.68	5.82	10.43
	December	797.4	251.8	454	1158	64.53	18.94	32.5	85.6	7.54	1.80	5	10.08
	January	739.1	273.5	331	1153	61.3	20.87	24.2	86.2	7	2.09	3.74	10.08
	February	761.1	266.2	371	1159	62.13	21.21	24.9	87.9	7.33	1.92	4.31	10.03
	March	887.3	253.9	548	1250	74.98	19.6	41.6	96.9	7.99	1.57	5.92	10.3
Configuration#3	October	820.6	253.2	504	1161	59.81	16.08	35.3	80.9	8.14	1.94	5.63	10.79
	November	880.4	254.2	539	1245	61.97	15.37	38.5	79.5	8.51	1.97	5.88	11.55
	December	798	251.8	455	1158	56.01	15.74	31.8	74.5	7.96	2.05	5.05	10.79
	January	739	273.4	331	1153	52.99	17.56	23.1	77.6	7.41	2.28	3.87	10.6
	February	761.4	266.6	371	1160	53.48	18.52	21.2	74.8	7.8	2.18	4.43	10.96
	March	888.2	253.9	549	1251	64.34	17.28	34.2	83.3	8.6	1.84	6.2	11.29

The SHA ranges from –45° to 75°, where negative values represent the pre-noon period, 0° corresponds to solar noon, and positive values indicate the post-noon period. Over the months, SR gradually increases as the SHA approaches 0°, reaching its peak between 0° and 15°. This period corresponds to the highest solar elevation and the lowest atmospheric attenuation. Beyond this range, SR progressively decreases with increasing SHA as the solar beam moves away from the meridian. Configurations #2 and #3 exhibit higher irradiance levels than Configuration #1, confirming that the reflector arrangement effectively enhances the interception of SR. Irradiance increases of approximately 40%–47% are recorded within the peak hour-angle range (0°–15°) for the reflector-assisted configurations compared to the reference panel.

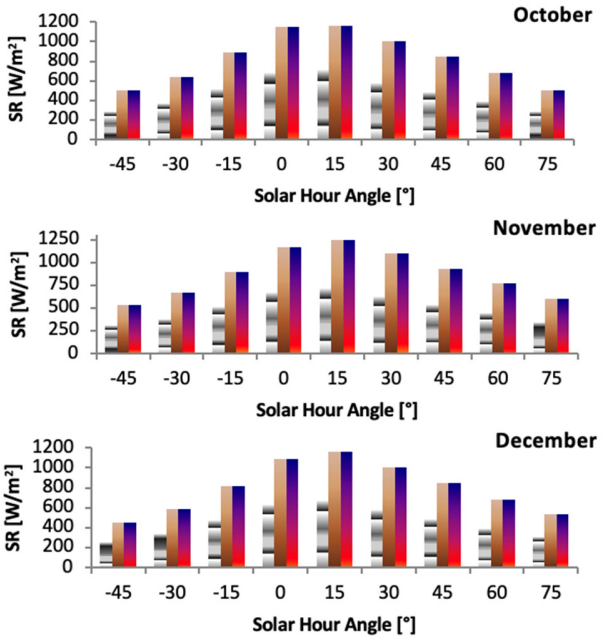

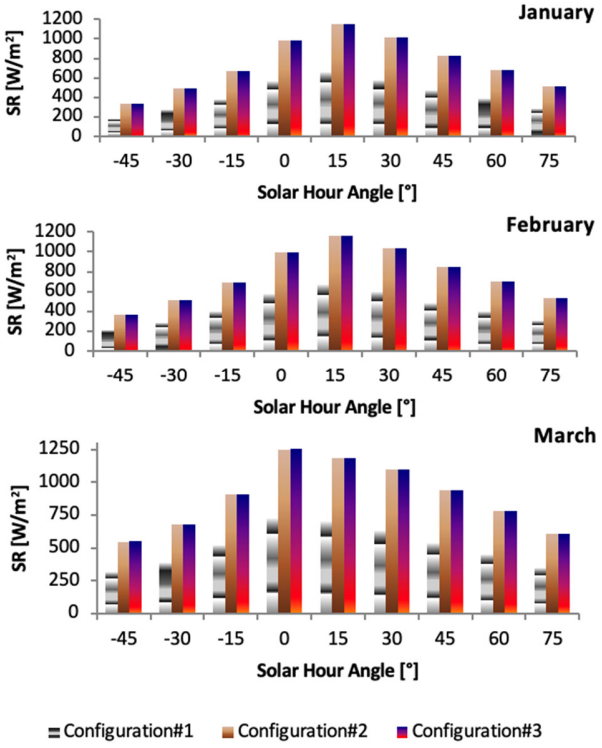

Fig. 4. SR versus SHA.

The seasonal variation further indicates that higher irradiance levels occur between October and March, mainly due to reduced cloud cover during this period. In contrast, lower irradiance levels are observed in December and January due to harmattan conditions. The nearly identical radiation intensity levels found for Configurations #2 and #3 across the full range of SHA suggest that the cooling system does not affect the intensity of the incident irradiance, indicating that the primary factor influencing performance variation is solely due to enhanced heating effects. Moreover, Figure 5 shows that the PV ST varies with the SHA (–45° to +75°) for each month. In

all months, the ST increases when the SHA is between 0° and +15°, where the sun is at its highest elevation, and decreases symmetrically at larger positive and negative hour angles, confirming that the influence of solar geometry on thermal behavior is strong.

Due to the increased irradiance induced by the reflected-induced optical concentration, Configuration #2 records the highest temperatures throughout the experimental campaign, while Configuration #3 displays lower temperatures owing to active cooling. Moreover, the peak temperature increase of Configuration #2 with respect to Configuration #1 amounts to about 27% in October, 26% in November, 25% in December, 24% in January, 26% in February, and 29% in March, which has been calculated for the close vicinity of the maximum hour-angle range. In contrast, the moderated temperature increase of around 11%–15% in Configuration #3 indicates the cooling system's ability to regulate the temperature rise while maintaining the increased solar input. There are seasonal variations in temperature, with lower temperatures in December and January due to harmattan conditions and higher temperatures in March due to clearer skies. In Figures 5 and 6, the results demonstrate a positive correlation between SR and ST: when solar irradiance is high, especially around solar noon, the PV module temperature tends to be higher because it absorbs more solar irradiance.

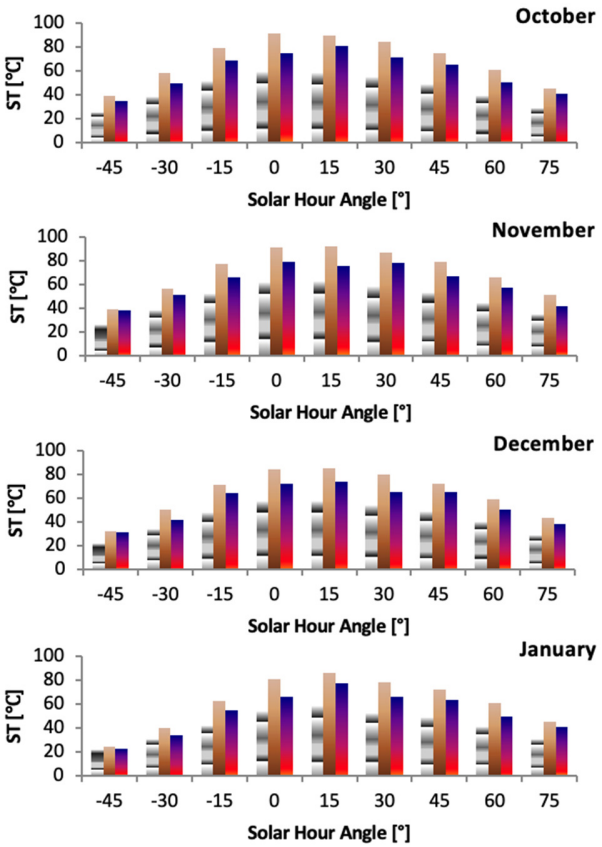

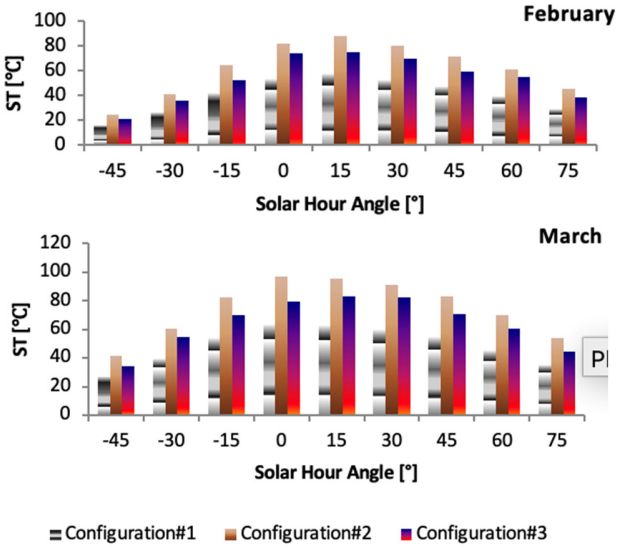

Fig. 5. ST versus SHA.

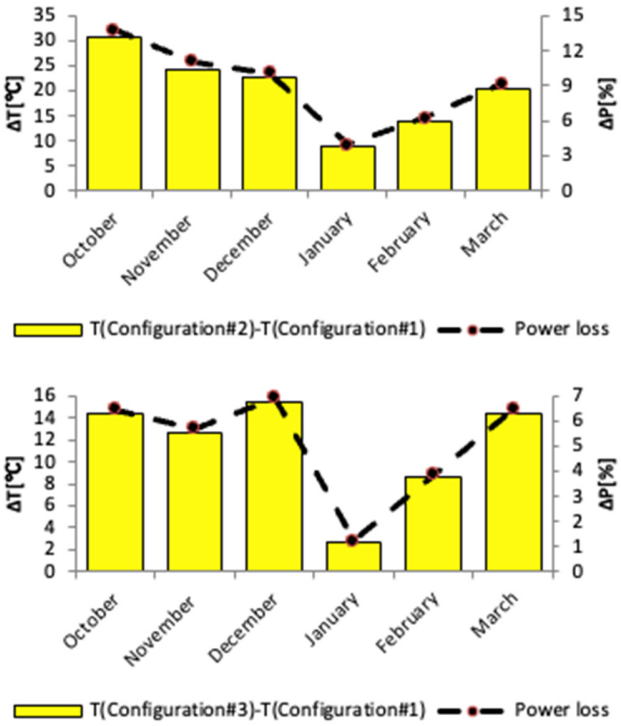

Fig. 6. Monthly temperature rise and power loss in PV configurations.

This is also documented in the literature. Authors in [43] showed that the temperature in a PV module tends to increase approximately linearly with increasing solar irradiation, thereby significantly affecting its electrical output. This trend was also observed in [44], where it was found that high solar irradiance levels contribute to elevated temperatures, necessitating improved cooling systems in high-temperature regions. This also confirms that solar irradiation is the main parameter determining PV operating temperature when ambient conditions are held constant [40].

In this study, the solar noon (0°) is taken as the reference hour angle when reporting temperature-based performance, since it corresponds to a maximum in solar irradiance and, hence, in thermal stress on the PV module. This is when reflector-induced irradiance enhancement and its associated temperature rise are the most significant, enabling thermal penalty quantification under the most adverse operating conditions. Thus, T_{ref} is the experimentally measured PV ST of the reference configuration (Configuration #1) at peak operating conditions (12:00 pm), while T_{PV} represents the measured temperature of the modified configurations at the same time. Using a coefficient of -0.45%/°C for polycrystalline modules, the increase in PV panel temperature in the reflector-only configuration ranges from 8.7 °C to 30.8 °C, resulting in a power loss of 3.9% to 13.9%, as shown in Figure 6. This could offset the increased irradiance levels. The use of the active cooling system in combination with the reflector demonstrates the system's potential to maximize the modules' overall electrical output by reducing module temperatures, thereby eliminating system losses.

Figure 7 illustrates the variation in electrical EP for the three PV configurations. The EP was calculated from the measured DC voltage and current using a voltmeter–ammeter method and analyzed as a function of the SHA over the six-month experimental period. For all months and configurations, the power output strongly depends on the SHA. Specifically, EP increases progressively from –45° and reaches peak values between 0° and +15°, after which it decreases at larger positive hour angles. This behavior follows the diurnal pattern of SR, where irradiance increases as the sun approaches its highest elevation and decreases as it moves toward the horizon. The results show that Configuration #2 consistently produces higher EP than Configuration #1 for all SHAs and seasons, confirming the positive effect of reflector-assisted optical concentration on power output. At peak SHAs, Configuration #2 achieves power gains of approximately 30%–40% compared with the reference system during most months of the year. However, this increase in power is accompanied by a significant rise in ST, as indicated by the thermal results. The elevated ST, particularly during peak hours, partially offsets the benefits of enhanced irradiance due to the negative temperature coefficient of PV modules. Configuration #3 exhibits the highest electrical output among the three configurations, particularly at peak SHAs. Although it receives nearly the same enhanced irradiance as Configuration #2, its power output is significantly higher. This improvement indicates that the active cooling system effectively reduces thermal losses by limiting the increase in module temperature.

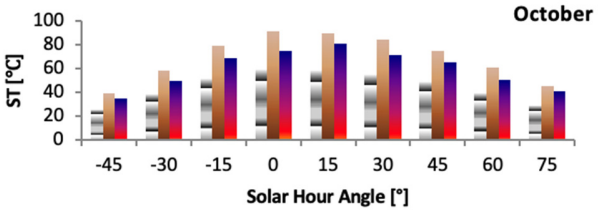

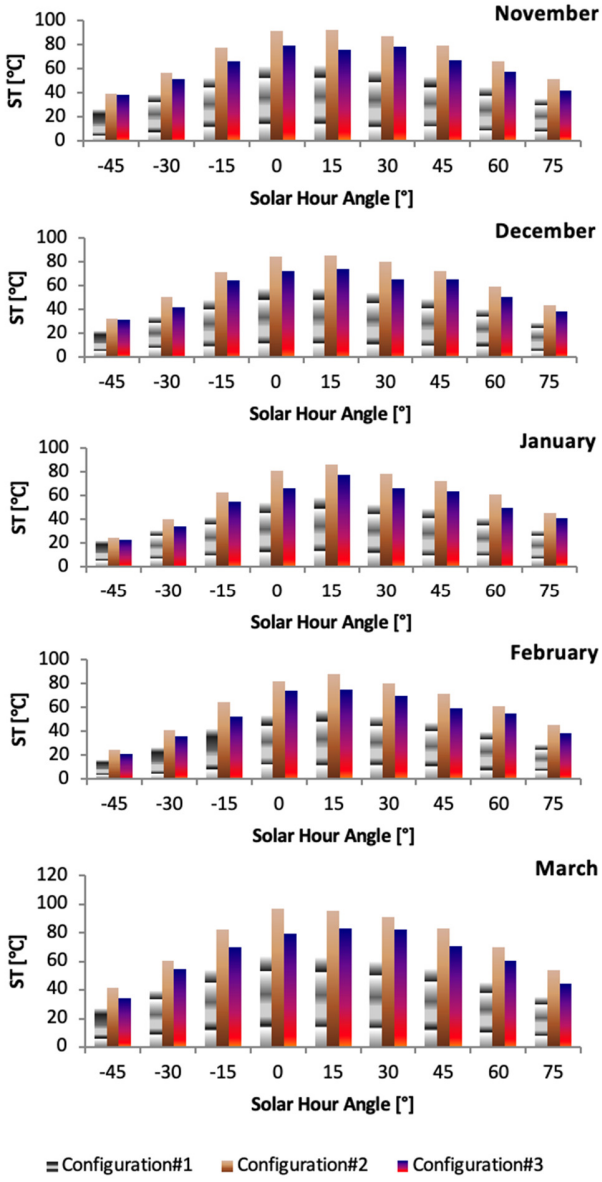

Fig. 7. ST versus SHA.

At the peak hour-angle range in March, Configuration #3 produces power outputs exceeding 11 W, compared to approximately 10.3 W for Configuration #2 and less than 8 W for Configuration #1. This demonstrates that maintaining high irradiance while controlling the ST leads to a net improvement in electrical performance. The results indicate a strong relationship among SR, ST, and power output. Higher SR generally increases power output due to enhanced photogenerated current. However, higher ST reduces the output voltage, which consequently suppresses the overall power output because of the negative temperature coefficient of PV modules. This behavior is evident in Configuration #2, where the higher solar irradiance increases power generation, but the simultaneous rise in ST partially offsets this gain. In contrast, Configuration #3 maintains lower ST while benefiting from

enhanced irradiance, thereby achieving the highest power output.

Furthermore, the variation in the power output with seasons also supports this correlation. The low power output during December and January corresponds to reduced SR and lower temperatures associated with the harmattan seasons, and the high power output in October and March corresponds to clearer skies and higher irradiance. Also, despite the lower irradiance during the harmattan periods, Configuration #3 still performs better than the other configurations, supporting the conclusion that cooling remains desirable even with reduced radiation. The outcomes are highly consistent with those of previous studies. Authors in [43] found that PV power output rises with irradiance intensity but falls with module temperature. In [44], it was shown that water cooling increases PV power output under high irradiation. Authors in [40] demonstrated that proper temperature management increases voltage stability and overall power output in PV, especially in regions with high temperatures. Authors in [45] concluded that it is not advisable to employ a cooling system in a reflector-assisted PV system due to reduced PV efficiency.

In this study, MLR is developed to estimate EP as a function of the MI, SR, and ST, as shown in:

Configuration#1

$$EP = 1.034 + 0.01 \cdot MI + 0.009 \cdot SR + 0.005 \cdot ST \quad (9)$$

Configuration#2

$$EP = 1.965 + 0.003 \cdot MI + 0.007 \cdot SR - 0.002 \cdot ST \quad (10)$$

Configuration#3

$$EP = 1.689 - 0.002 \cdot MI + 0.008 \cdot SR - 0.001 \cdot ST \quad (11)$$

Moreover, Figures 8-10 illustrate how MI, SR, and ST affect EP. The EP contour plots show the impacts of parameter interactions. The interaction effect between the parameters was represented in each contour plot. The contour areas help explain how the MI, SR, and ST vary with changes in experimental conditions. The number written on each contour area indicates the EP in the specified conditions. These contour plots demonstrated that the interaction effects of all parameters were considerable.

G. Large-Scale Performance Projection and Scaling Methodology

To validate the results derived from the experimental analysis of the 10 W PV modules studied in this investigation, a performance-scaling methodology with sound foundations in PV modeling was used. Conducting comprehensive experimental analyses for large-capacity PV systems and modules would be impractical and potentially cost- and space-prohibitive in the contemporary setting; as a result, several scaling theories were developed that have sound foundations in irradiance-temperature-power relationships. Derived from the linear relationship between the photoelectric power and the solar irradiance and active area of the PV module, along with several temperature correction multipliers for estimating the associated losses during actual operating conditions, this model has been successfully utilized in previous experimental and theoretical studies to validate the potential feasibility of large-scale PV systems.

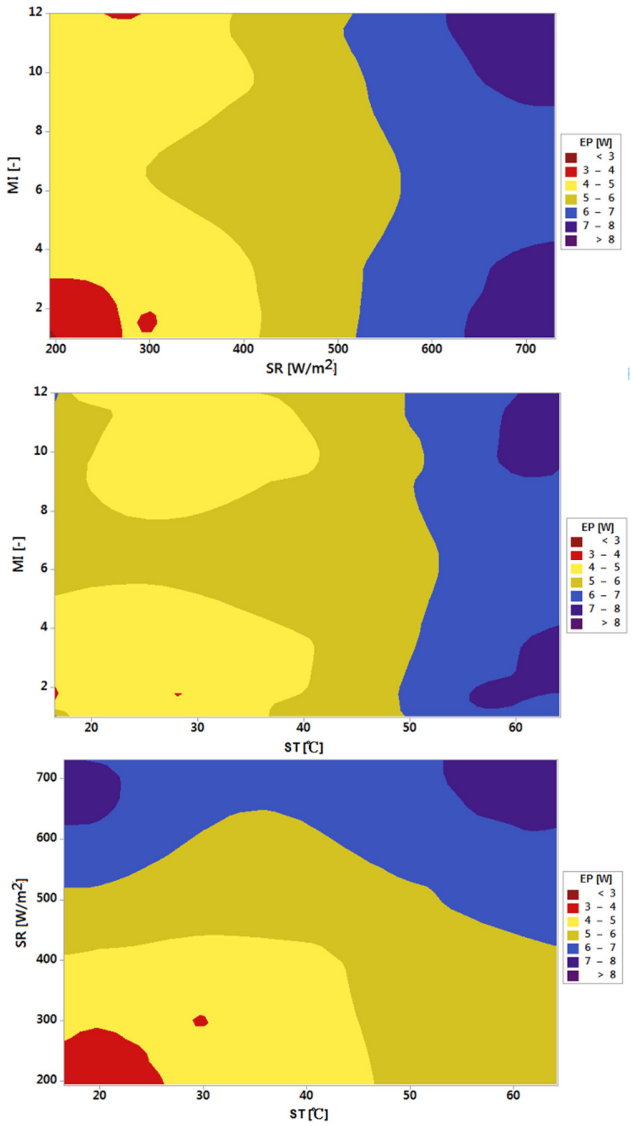

Fig. 8. 3D surface plot of PV power output as a function of MI, solar irradiance, and ST for Configuration#1.

1) Scaling Power with Irradiance

A PV cell's output is a constant proportion of the irradiance if the temperature remains constant, as given in:

$$EP \propto SR \quad (4)$$

This is a linear relationship whereby an increase in SR leads to a direct proportional rise in current and power [46].

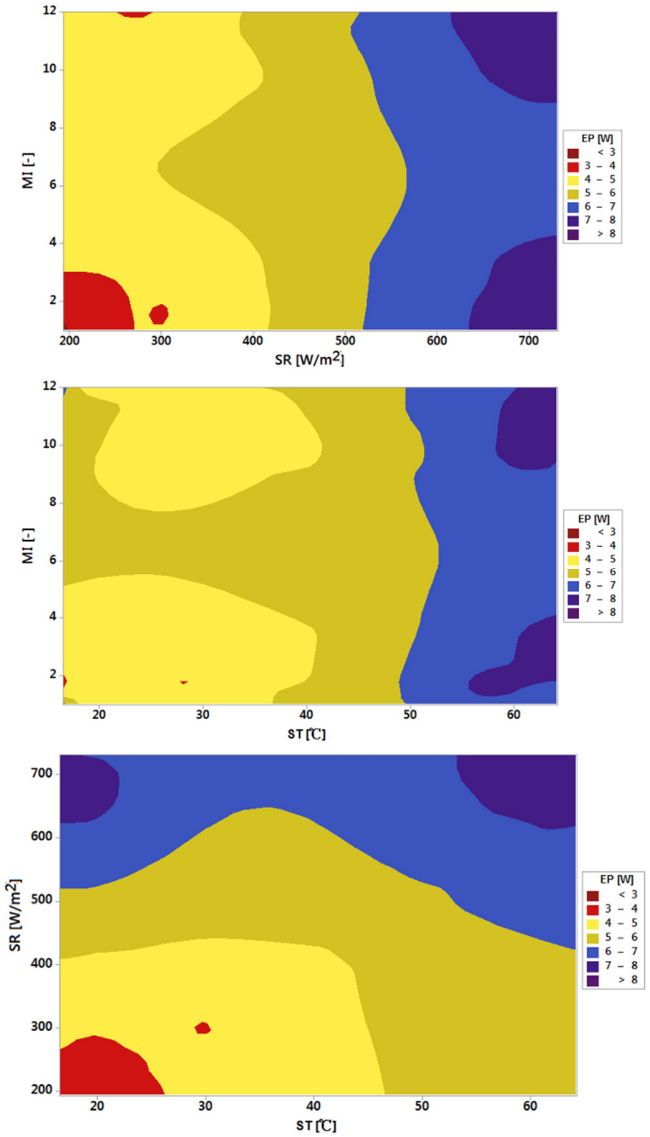

Fig. 9. 3D surface plot of PV power output as a function of MI, solar irradiance, and ST for Configuration#2.

2) Temperature Correction for Power Output

The PV power also depends on operating temperature and can be expressed as:

$$P(T) = P_{STC}[1 - \beta_P(T - T_{STC})] \quad (5)$$

where $P(T)$ is the power at operating temperature, P_{STC} is the power at STC (1000 W/m² and 25 °C), and β_P is the temperature coefficient of power (%/°C).

According to [47], (5) captures the negative temperature impact on PV output and is one of the most used expressions within PV performance modeling.

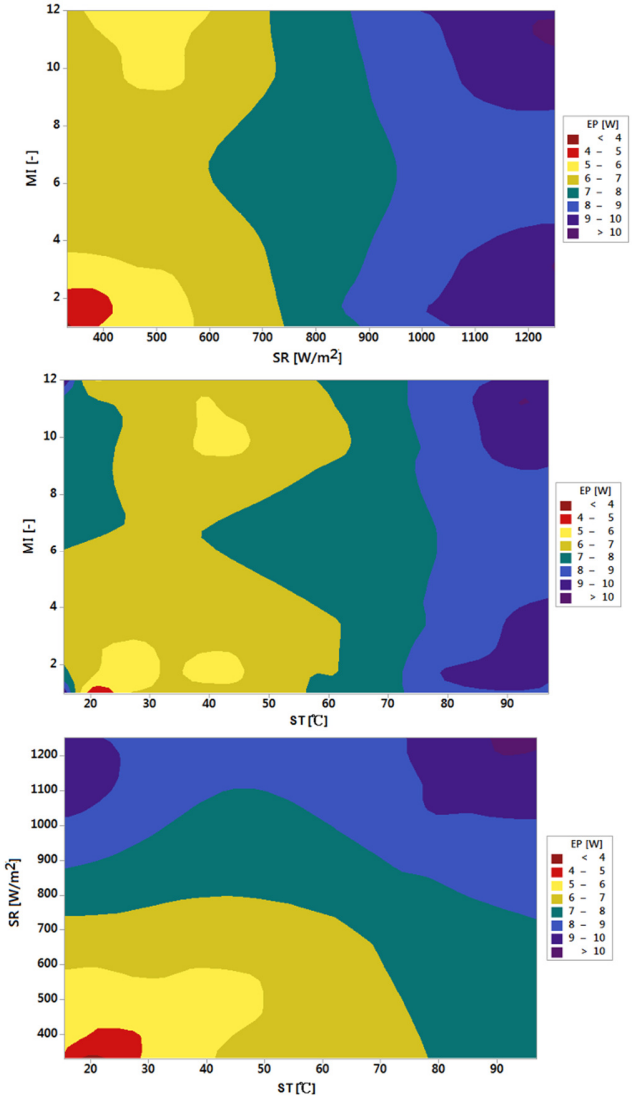

Fig. 10. 3D surface plot of PV power output as a function of MI, solar irradiance, and ST for Configuration#3.

1). Area Scaling Law (Linear with Panel Area)

For a larger system composed of more PV modules (with the same technology and tilt):

$$EP_{large} = EP_{small} \times \frac{A_{large}}{A_{small}} \quad (6)$$

where EP_{small} is the power measured from the 10 W panel, A_{large} is a planned large system area, and A_{small} is the area of the panel (10 W).

The above scaling law assumes uniform irradiation and temperature conditions across the panels. Similar scale approaches are reported in the design studies of PV systems, where small-scale measurements are extrapolated to utility-scale systems [48]. The annual energy output was determined using a scaling and extrapolation technique based on the six-month test period corresponding to the most effective configuration (Configuration #3). The calculation assumes a free rooftop space of 1000 m² with an effective factor of 80%,

resulting in an active surface area of 800 m², homogeneously covered with identical modules having equivalent thermal and electrical properties. It was also assumed that the power output measured during the experiments for a given solar hour is a fair representation of energy performance during clear-sky conditions in Kano State, and that inverter loss correction is considered with a fixed DC-to-AC efficiency of 95%. The daily energy output was determined by integrating the hourly energy output. In contrast, the monthly energy output was determined as the product of the daily energy output and the number of clear days in each month. Because the six-month test period spanned the experiments from October to March, a yearly energy output was determined based on symmetric performance conditions assumed for a comparable six-month period in a year.

Moreover, a sensitivity analysis was conducted to examine the system's viability by varying the assumptions within realistic ranges, as shown in Table III. This was done to confirm the robustness of the large-scale performance projection and the assumptions of the given uniform irradiance, symmetric annual performance, and inverter efficiency. Inverter efficiencies range from 90% to 97%. The asymmetric performance caused by the seasonal lack of solar power was anticipated by adjusting the inverter efficiencies within ±10% to 15% of the actual six-month inverter performance measurement. Additionally, non-uniform irradiance levels resulting from dust accumulation, partial shade, and temperature gradients across the system location were estimated to vary by up to 10%. The yearly energy yield ranges from 160 MWh to 215 MWh, and the findings fall within the benchmark range of 187 MWh, demonstrating that the technology has been successfully implemented while maintaining system viability.

TABLE III. SENSITIVITY ANALYSIS OF KEY ASSUMPTIONS USED IN LARGE-SCALE PV PERFORMANCE PROJECTION

Parameter varied	Assumed nominal value	Variation range	Impact on annual energy yield
Inverter efficiency	95%	90%–97%	±5%–7%
Seasonal symmetry (six-month extrapolation)	Symmetric annual performance	±10%–15%	±10%–15%
Effective irradiance uniformity	Uniform irradiance	±10%	±8%–10%
Combined effect	-	-	160 MWh/year –215 MWh/year

III. CONCLUSIONS

This work experimentally demonstrated that the performance of a PV system operating in hot climates can be significantly improved by combining solar reflectors and active cooling. Incident SR was increased by as much as 47% in the reflector-assisted configurations, indicating the viability of low-cost optical concentration methods to enhance irradiance interception. However, ST rose significantly by up to ~29% when a reflector-only configuration was applied, which, because of the negative temperature coefficient of PV modules, somewhat dampened the electrical gains. The integration of an active water-cooling system alleviated these thermal penalties and limited the temperature rise to about 11%-15%, while preserving the enhanced irradiance. These factors combined to realize the highest electrical output from the reflector-cooling configuration across all seasons and SHAs, including peak power over 11 W compared to below 8 W for the unmodified panel. The scaling analysis performed indicated that such performance gains can result in an estimated annual energy yield of approximately 187 MWh for a 1000 m² installation in Nigeria's northern region. This evidence demonstrates that the hybrid optical-thermal management technique is an effective means of enhancing the efficiency of PV cells in high-temperature environments. Despite these improvements, the current work still has some significant drawbacks. Active cooling increases water consumption and complicates the system, and the accumulation of dust, cooling circuit maintenance, and the slow deterioration of reflector optical qualities can all affect long-term performance. These factors were not explicitly quantified here and might influence long-term performance and economic viability.

IV. FUTURE WORK

Future studies should focus on the effects of dust soiling, reflector durability, maintenance needs, and water usage through extended outdoor testing. Reducing energy and water consumption can be achieved, in part, by adding temperature sensors and implementing control algorithms for cooling flow rates. Using new reflector materials and coatings, geometries designed for varied solar-tracking trajectories, nanofluids or phase-change-based cooling systems, and other contemporary cooling media can contribute to achieving further performance gains. Furthermore, the potential to exploit natural convective cooling while addressing land-use issues is presented by extending the proposed concept of reflector and cooling systems to platforms for floating solar systems. To validate the scalability and sustainability of the proposed enhancement technique in developing nations and high-temperature applications, techno-economic and life-cycle assessments that account for water use, pumping energy, maintenance costs, and environmental impact are essential. Moreover, long-term measurements conducted outdoors should be integrated with regional meteorological data to account for seasonal asymmetry. This will enhance the prediction of annual energy yields. Finally, infrared thermography will be used in future studies to measure ST uniformity and identify hot spots during cooling system operation.

REFERENCES

[1] M. B. Ben Hamida, A. Khelifa, M. E. Hadi Attia, and M. M. Abdel-Aziz, "Maximizing energy output in PVT systems with triangular-finned solar air collectors," *Applied Thermal Engineering*, vol. 278, Nov. 2025, Art. no. 127247, https://doi.org/10.1016/j.applthermaleng.2025.127247.

[2] M. E. Hadi Attia, M. M. Abdel-Aziz, and A. Khelifa, "A numerical approach to enhance the performance of double-pass solar collectors with finned photovoltaic/thermal integration," *Applied Thermal Engineering*, vol. 268, June 2025, Art. no. 125974, https://doi.org/10.1016/j.applthermaleng.2025.125974.

[3] M. E. H. Attia, A. E. Kabeel, A. Khelifa, M. M. Abdel-Aziz, R. Sathyamurthy, and W. M. El-Maghlany, "Optimal air cooling gap width at the top of the PVT: thermal and electrical efficiency analysis," *Journal of Thermal Analysis and Calorimetry*, vol. 150, no. 3, pp. 2047–2058, Feb. 2025, https://doi.org/10.1007/s10973-024-13882-2.

[4] M. E. H. Attia, A. E. Kabeel, A. Khelifa, M. Abdelgaied, M. Arıcı, and M. M. Abdel-Aziz, "Performance enhancement of PVT modules using bi-fluid (air/CuO–water-based nanofluid) and fins: energy and exergy analysis," *Clean Technologies and Environmental Policy*, vol. 27, no. 9, pp. 4541–4559, Sept. 2025, https://doi.org/10.1007/s10098-025-03149-1.

[5] E. Imik and M. Yilmaz, "A Numerical Investigation on the Performance and Sustainability Analysis of Conventional and Finned Air-Cooled Solar Photovoltaic Thermal (PV/T) Systems," *Sustainability*, vol. 17, no. 23, Nov. 2025, https://doi.org/10.3390/su172310638.

[6] Y. El Alami, A. Ameur, M. Benhmida, A. Rabhi, and E. Baghaz, "Performance evaluation of different new channel box photovoltaic thermal systems," *Journal of Cleaner Production*, vol. 478, Nov. 2024, Art. no. 143953, https://doi.org/10.1016/j.jclepro.2024.143953.

[7] Y. El Alami *et al.*, "Experimental-numerical comparative study of performance and cost-effectiveness of partially- and fully-cooled photovoltaic thermal systems," *Case Studies in Thermal Engineering*, vol. 73, Sept. 2025, Art. no. 106660, https://doi.org/10.1016/j.csite.2025.106660.

[8] Y. El Alami, H. E. Achouby, E. Baghaz, C. Hajjaj, and R. Nasrin, "An innovative photovoltaic thermal system with direct water-cell contact: energy, exergy, and sustainability analysis," *Solar Energy*, vol. 300, Nov. 2025, Art. no. 113827, https://doi.org/10.1016/j.solener.2025.113827.

[9] M. M. Abdel-Aziz and A. A. ElBahloul, "Optimization of different composite sorption materials and their thickness for enhanced PV cooling performance: A multiphysics simulation approach," *Solar Energy Materials and Solar Cells*, vol. 285, June 2025, Art. no. 113554, https://doi.org/10.1016/j.solmat.2025.113554.

[10] Y. El Alami *et al.*, "Experimental-Numerical Investigation of the Photovoltaic Thermal System with Polypropylene Heat Exchanger: Case in Morocco," *IET Renewable Power Generation*, vol. 19, no. 1, 2025, Art. no. e70041, https://doi.org/10.1049/rpg2.70041.

[11] Y. Bannour, Y. El Alami, R. Nasrin, N. E. Moussaoui, B. Elhadi, and A. Faiz, "Numerical Optimization of Fin Configurations in Phase Change Material Systems for Improving Solar Panel Cooling and Electrical Efficiency," *Energy Storage*, vol. 7, no. 5, 2025, Art. no. e70241, https://doi.org/10.1002/est2.70241.

[12] Y. El Alami, E. Baghaz, R. Nasrin, S. Padmanaban, and M. Louzazni, "Numerical approach of an advanced hybrid photovoltaic thermal system based on exergy, energy, enviro-economic, and sustainability factors," *Results in Engineering*, vol. 27, Sept. 2025, Art. no. 106342, https://doi.org/10.1016/j.rineng.2025.106342.

[13] Y. El Alami, B. Zohal, R. Nasrin, M. Benhmida, A. Faize, and E. Baghaz, "Solar thermal, photovoltaic, photovoltaic thermal, and photovoltaic thermal phase change material systems: A comprehensive reference guide," *International Communications in Heat and Mass Transfer*, vol. 159, Dec. 2024, Art. no. 108135, https://doi.org/10.1016/j.icheatmasstransfer.2024.108135.

[14] M. Asvad, M. Gorji, and A. Mahdavi, "Performance analysis of a solar module with different reflectors and cooling flow fields," *Applied Thermal Engineering*, vol. 219, Jan. 2023, Art. no. 119469, https://doi.org/10.1016/j.applthermaleng.2022.119469.

[15] A. E. Kabeel, M. Abdelgaied, and R. Sathyamurthy, "A comprehensive investigation of the optimization cooling technique for improving the performance of PV module with reflectors under Egyptian conditions," *Solar Energy*, vol. 186, pp. 257–263, July 2019, https://doi.org/10.1016/j.solener.2019.05.019.

[16] B. M. Ziapour, V. Palideh, and F. Mokhtari, "Performance improvement of the finned passive PVT system using reflectors like removable insulation covers," *Applied Thermal Engineering*, vol. 94, pp. 341–349, Feb. 2016, https://doi.org/10.1016/j.applthermaleng.2015.10.143.

[17] A. E. Kabeel, M. Abdelgaied, R. Sathyamurthy, and A. Kabeel, "A comprehensive review of technologies used to improve the performance of PV systems in a view of cooling mediums, reflectors design, spectrum splitting, and economic analysis," *Environmental Science and Pollution Research*, vol. 28, no. 7, pp. 7955–7980, Feb. 2021, https://doi.org/10.1007/s11356-020-11008-3.

[18] M. Aziz-ul Huq, M. I. Hossain, and M. M. Rahman, "Effect of flat reflectors on the performance of photovoltaic modules," in Collection of Technical Papers. 35th Intersociety Energy Conversion Engineering Conference and Exhibit (IECEC) (Cat. No.00CH37022), July 2000, vol. 1, pp. 161–168 vol.1, https://doi.org/10.1109/IECEC.2000.870667.

[19] E. A. Setiawan and K. Dewi, "Impact of Two Types Flat Reflector Materials on Solar Panel Characteristics," *International Journal of Technology*, vol. 4, no. 2, July 2013, Art. no. 188, https://doi.org/10.14716/ijtech.v4i2.108.

[20] V. N. Palaskar, S. P. Deshmukh, and A. B. Pandit, "Design and Performance Analysis of Reflectors Attached to Commercial PV Module," *International Journal of Renewable Energy Research*, vol. 4, no. 1, pp. 240–245, Mar. 2014, [Online]. Available: https://dergipark.org.tr/en/pub/ijrer/article/168158.

[21] N. K. Kasim, A. F. Atwan, and F. M. Eliewi, "Improve the performance of solar modules by reflectors," *Journal of Physics: Conference Series*, vol. 1032, no. 1, Feb. 2018, Art. no. 012031, https://doi.org/10.1088/1742-6596/1032/1/012031.

[22] M. A. Khan *et al.*, "Design of a Building-Integrated Photovoltaic System with a Novel Bi-Reflector PV System (BRPVS) and Optimal Control Mechanism: An Experimental Study," *Electronics*, vol. 7, no. 7, July 2018, https://doi.org/10.3390/electronics7070119.

[23] B. J. Huang and F. S. Sun, "Feasibility study of one axis three positions tracking solar PV with low concentration ratio reflector," *Energy Conversion and Management*, vol. 48, no. 4, pp. 1273–1280, Apr. 2007, https://doi.org/10.1016/j.enconman.2006.09.020.

[24] M. Mawoli, H. N. Yayha, B. G. Danshehu, M. L. Muhammad, and A. S. Bature, "Development and Performance Evaluation of Solar Photovoltaic Module's Surface-to-Rear Temperature Controlled Valve for Cooling Application," *Nigerian Journal of Technological Development*, vol. 17, no. 1, pp. 20–27, Apr. 2020, https://doi.org/10.4314/njtd.v17i1.3.

[25] I. A. Tukur *et al.*, "Performance Evaluation of Reflectors and Cooling System on Photovoltaic System in Kano Northwest Nigeria," *FUDMA JOURNAL OF SCIENCES*, vol. 7, no. 3, pp. 72–76, July 2023, https://doi.org/10.33003/fjs-2023-0703-1776.

[26] K. R. Awai, P. King, K. Patchigolla, and S. M. Jain, "Investigating Performance of Hybrid Photovoltaic–Thermal Collector for Electricity and Hot Water Production in Nigeria," *Energies*, vol. 17, no. 11, June 2024, https://doi.org/10.3390/en17112776.

[27] A. T. Ibrahim, A. A. Abdullahi, A. T. Mustapha, J. Nura, and A. Bala, "Performance Evaluation of Solar Panel with Reflector Using Nano Fluids," *ARID ZONE JOURNAL OF ENGINEERING, TECHNOLOGY AND ENVIRONMENT*, vol. 21, no. 1, pp. 1–12, Mar. 2025, [Online]. Available: https://azojete.com.ng/index.php/azojete/article/view/1004.

[28] C. S. Solanki, C. S. Sangani, D. Gunashekar, and G. Antony, "Enhanced heat dissipation of V-trough PV modules for better performance," *Solar Energy Materials and Solar Cells*, vol. 92, no. 12, pp. 1634–1638, Dec. 2008, https://doi.org/10.1016/j.solmat.2008.07.022.

[29] C. S. Sangani and C. S. Solanki, "Experimental evaluation of V-trough (2 suns) PV concentrator system using commercial PV modules," *Solar Energy Materials and Solar Cells*, vol. 91, no. 6, pp. 453–459, Mar. 2007, https://doi.org/10.1016/j.solmat.2006.10.012.

[30] D. G. Burkhard, G. L. Strobel, and D. R. Burkhard, "Flat-sided rectilinear trough as a solar concentrator: an analytical study," *Applied Optics*, vol. 17, no. 12, pp. 1870–1883, June 1978, https://doi.org/10.1364/AO.17.001870.

[31] Y. A. Cengel and A. J. (Afshin J. Ghajar, *Heat and mass transfer : fundamentals and applications*, 6th edition in SI unites. McGraw-Hill, 2020.

[32] P. J. Pritchard and J. W. Mitchell, Fox and McDonald's Introduction to Fluid Mechanics, 9th Edition. Wiley, 2015.

[33] T. L. Bergman, *Fundamentals of Heat and Mass Transfer*. John Wiley & Sons, 2011.

[34] J. Kiijarvi, "Darcy Friction Factor Formulae in Turbulent Pipe Flow," June 2011, Art. no. 110727.

[35] T. Limboonruang, M. Oyinlola, D. Harmanto, and N. Phunapai, "Optimizing the configuration of external fins of solar receiver tubes for

the solar parabolic trough collector," *Applied Thermal Engineering*, vol. 263, Mar. 2025, Art. no. 125317, https://doi.org/10.1016/j.applthermaleng.2024.125317.

[36] A. Ahmed, A. Fouda, H. F. Elattar, K. Alnamasi, and A. M. A. Alsharif, "Advancing photovoltaic thermal module efficiency through optimized heat sink designs," *Applied Thermal Engineering*, vol. 271, July 2025, Art. no. 126241, https://doi.org/10.1016/j.applthermaleng.2025.126241.

[37] S. Rahmanian and A. Hamzavi, "Effects of pump power on performance analysis of photovoltaic thermal system using CNT nanofluid," *Solar Energy*, vol. 201, pp. 787–797, May 2020, https://doi.org/10.1016/j.solener.2020.03.061.

[38] B. Menacer, N. E. H. Baghdous, S. Narayan, M. Al-lehaibi, L. Osorio, and V. Tuninetti, "Efficiency Enhancement of Photovoltaic Panels via Air, Water, and Porous Media Cooling Methods: Thermal–Electrical Modeling," *Sustainability*, vol. 17, no. 14, July 2025, https://doi.org/10.3390/su17146559.

[39] E. Radziemska, "The effect of temperature on the power drop in crystalline silicon solar cells," *Renewable Energy*, vol. 28, no. 1, pp. 1–12, Jan. 2003, https://doi.org/10.1016/S0960-1481(02)00015-0.

[40] S. Dubey, J. N. Sarvaiya, and B. Seshadri, "Temperature Dependent Photovoltaic (PV) Efficiency and Its Effect on PV Production in the World – A Review," *Energy Procedia*, vol. 33, pp. 311–321, Jan. 2013, https://doi.org/10.1016/j.egypro.2013.05.072.

[41] "Temperature Coefficient Loss Calculator | SolarMathLab." https://solarmathlab.com/output/temperature-coefficient-loss.html.

[42] Y. Kassem, H. Gökçekuş, H. Çamur, and E. Esenel, "Application of artificial neural network, multiple linear regression, and response surface regression models in the estimation of monthly rainfall in Northern Cyprus," *Desalination and Water Treatment*, vol. 215, pp. 328–346, Mar. 2021, https://doi.org/10.5004/dwt.2021.26525.

[43] E. Skoplaki and J. A. Palyvos, "On the temperature dependence of photovoltaic module electrical performance: A review of efficiency/power correlations," *Solar Energy*, vol. 83, no. 5, pp. 614–624, May 2009, https://doi.org/10.1016/j.solener.2008.10.008.

[44] H. Bahaidarah, A. Subhan, P. Gandhidasan, and S. Rehman, "Performance evaluation of a PV (photovoltaic) module by back surface water cooling for hot climatic conditions," *Energy*, vol. 59, pp. 445–453, Sept. 2013, https://doi.org/10.1016/j.energy.2013.07.050.

[45] A. Hasan, S. J. McCormack, M. J. Huang, and B. Norton, "Evaluation of phase change materials for thermal regulation enhancement of building integrated photovoltaics," *Solar Energy*, vol. 84, no. 9, pp. 1601–1612, Sept. 2010, https://doi.org/10.1016/j.solener.2010.06.010.

[46] A. Bala, M. B. Alao, A. O. Oyedun, O. O. Alabi, and M. Adamu, "Performance Evaluation of a Solar Photovoltaic (PV) Module at Different Solar Irradiance," *International Journal of Engineering and Applied Sciences*, vol. 16, no. 2, pp. 63–75, July 2024, https://doi.org/10.24107/ijeas.1430556.

[47] D. Xiao and T. Liu, "Optimized photovoltaic system for improved electricity conversion," *International Journal of Low-Carbon Technologies*, vol. 17, pp. 456–461, Feb. 2022, https://doi.org/10.1093/ijlct/ctab103.

[48] G. Li, Y. Lu, S. Shittu, and X. Zhao, "Scale effect on electrical characteristics of CPC-PV," *Energy*, vol. 192, Feb. 2020, Art. no. 116726, https://doi.org/10.1016/j.energy.2019.116726.